Original Article

JCBFM

Journal of Cerebral Blood Flow & Metabolism
2022, Vol. 42(2) 315–328

DOI: 10.1177/0271678X211045848
journals.sagepub.com/home/jcbfm
SAGE

Cerebral haemodynamic response to somatosensory stimulation in preterm lambs and 7–10-day old lambs born at term: Direct synchrotron microangiography assessment

Ishmael M Inocencio[1,2,*], Nhi T Tran[1,2,3,*], Shinji Nakamura[1,4], Song J Khor[1,2], Manon Wiersma[1,2], Katja Stoecker[1,2], Anton Maksimenko[5], Graeme R Polglase[1,6], David W Walker[1,3], James T Pearson[7,8] and Flora Y Wong[1,2,9]

Abstract

Neurovascular coupling has been well-defined in the adult brain, but variable and inconsistent responses have been observed in the neonatal brain. The mechanisms that underlie functional haemodynamic responses in the developing brain are unknown. Synchrotron radiation (SR) microangiography enables *in vivo* high-resolution imaging of the cerebral vasculature. We exploited SR microangiography to investigate the microvascular changes underlying the cerebral haemodynamic response in preterm ($n = 7$) and 7–10-day old term lambs ($n = 4$), following median nerve stimulation of 1.8, 4.8 and 7.8 sec durations.

Increasing durations of somatosensory stimulation significantly increased the number of cortical microvessels of $\leq$200 μm diameter in 7–10-day old term lambs ($p < 0.05$) but not preterm lambs where, in contrast, stimulation increased the diameter of cerebral microvessels with a baseline diameter of $\leq$200 μm. Preterm lambs demonstrated positive functional responses with increased oxyhaemoglobin measured by near infrared spectroscopy, while 7–10-day old term lambs demonstrated both positive and negative responses. Our findings suggest the vascular mechanisms underlying the functional haemodynamic response differ between the preterm and 7–10-day old term brain. The preterm brain depends on vasodilatation of microvessels without recruitment of additional vessels, suggesting a limited capacity to mount higher cerebral haemodynamic responses when faced with prolonged or stronger neural stimulation.

Keywords

Cerebral haemodynamic response, neurovascular coupling, preterm, newborn, synchrotron microangiography

Received 3 May 2021; Revised 15 August 2021; Accepted 22 August 2021

[1]The Ritchie Centre, The Hudson Institute of Medical Research, Melbourne, Australia
[2]Department of Paediatrics, Monash University, Melbourne, Australia
[3]School of Health & Biomedical Sciences, RMIT University, Melbourne, Australia
[4]Department of Pediatrics, Faculty of Medicine, Kagawa University, Kagawa, Japan
[5]Imaging and Medical Beamline, Australian Synchrotron, ANSTO, Melbourne, Australia
[6]Department of Obstetrics and Gynaecology, Monash University, Melbourne, Australia
[7]Department of Cardiac Physiology, National Cerebral and Cardiovascular Centre, Osaka, Japan
[8]Monash Biomedicine Discovery Institute and Department of Physiology, Monash University, Melbourne, Australia
[9]Monash Newborn, Monash Children's Hospital, Melbourne, Australia

*Co-first authors who contributed equally to this work.

Corresponding author:
Flora Wong, Monash Children's Hospital, Level 5, 246 Clayton Rd, Clayton, Victoria 3168, Australia.
Email: flora.wong@monash.edu

Introduction

Increases in local neuronal activity result in localised increase of cerebral blood flow (CBF), a process known as neurovascular coupling.[1] The influx of oxygenated, arterial blood temporarily exceeds the consumption of oxygen by the tissue, leading to localised increases in oxygenation which can be detected as an increase in oxy-haemoglobin (oxyHb) and a decrease in deoxy-haemoglobin (deoxyHb) by functional near-infrared spectroscopy (fNIRS), or as a positive blood oxygen level-dependent (BOLD) signal by functional magnetic resonance imaging (fMRI). This typical haemodynamic response in the adult brain is called 'functional hyperaemia', which implies an increased CBF presumably due to cerebral vasodilatation.

Interestingly, in early postnatal life, whether after preterm or term birth, some neonatal haemodynamic functional studies have reported the adult-like positive responses,[2–6] but other studies suggest somatosensory stimulation induces a decrease in BOLD signal (often termed 'negative BOLD') during early human infancy.[7–9] Similarly, negative responses have been reported using fNIRS in newborn rodents and human neonates, with decreases in cerebral oxyHb and variable changes in the deoxyHb upon neural stimulation.[10–13] Interpretation of results is often confounded by the different study protocols, methods used for neuronal stimulation, heterogeneity of patients and their clinical conditions. The physiological origin of the variable and negative responses in the immature brain remain controversial, including: increase in neuronal activity and cerebral oxygen consumption without a compensatory increase in CBF; a decrease in CBF due to the normal redistribution and so-called 'haemodynamic steal' of blood towards an adjacent activated cortical region; or vasoconstriction in the area of neuronal activity.[14,15]

Notably, both the fNIRS and fMRI signals are based on changes in the amount of oxygenated and deoxygenated haemoglobin i.e., the balance between cerebral oxygen delivery and consumption, however neither are an actual assessment or measurement of vascular conductance or CBF. The underlying mechanisms of the functional haemodynamic response in the developing brain where angiogenesis is still ongoing and much of the vascular bed is structurally immature, are still unclear. Apart from changes in vessel calibre (vasodilation/vasoconstriction), recruitment of underperfused microvessels may also contribute to CBF changes.[16] Nevertheless, *in vivo* assessments of the intracerebral vasculature and vascular control of CBF remain challenging, especially at the level of the smallest intracerebral arterioles within the brain parenchyma which control the regional haemodynamic response.[17] Conventional cerebral angiography can detect vessels with diameters as small as 200 μm.[18] However, adult post-mortem analysis has revealed the diameters of cortical arteries and arterioles to be between 20–750 μm,[19] though these measurements may not be comparable to *in vivo* vessel diameters given that vessels collapse significantly upon cessation of cardiac output and blood flow, and there is significant shrinking of tissue due to histological processing.

Synchrotron radiation (SR) microangiography offers novel non-invasive high-resolution imaging in live animals that can detect dynamic changes in regional vascular networks. SR microangiography is useful for *in vivo* repeated real-time imaging of microvessel internal diameter and numbers under different physiological or pathological conditions.[17,20] In general, high-resolution SR microangiography has routinely been attainable for small imaging fields-of-view, visualizing cerebral microvessels down to 20–30 μm in diameter in small animal investigations.[18] We recently demonstrated the use of SR microangiography to study cerebral haemodynamics in the preterm lamb where the brain size is relatively small,[21] and comparable in size and structure to the human neonatal brain.[22] Indeed, preterm sheep have been used extensively to define the pathophysiology of the preterm cerebral circulation,[23] and we have previously used the NIRS technique in fetal, preterm and term lambs to study cerebral haemodynamic responses provoked by somatosensory stimulation.[16,24,25] In this study, we exploited the potential of monochromatic SR microangiography together with NIRS to study functional cerebral haemodynamics in preterm and 7–10-day old term lambs for the first time. We aimed to investigate the microvascular changes underlying the cerebral haemodynamic responses in the immature brain. Through analyses of cerebral vessel internal diameter and vessel counts in the SR microangiograms, we assessed the acute perfusion changes in intraparenchymal cerebral vasculature in preterm and 7–10-day old term lambs during median nerve stimulations.

Methods

Animal ethics

All experiments were performed at the Imaging and Medical beamline of the Australian Synchrotron, (IMBL) in Melbourne, Australia. Merino-Border Leicester cross pregnant ewes and newborn lambs were supplied by the Monash Animal Research Platform. Experiments were approved by the Monash Medical Centre and Australian Synchrotron Animal Ethics Committees (AS 2016–005, proposals M11046, M12906 & M12664). Experiments were conducted in accordance with the Australian Code of Practice for

the care and use of Animals for Scientific Purposes established by the National Health and Medical Research Council of Australia. All animal experiments complied with the ARRIVE guidelines.[26]

Surgery and lamb instrumentation

Preterm and 7–10-day old term lambs were used in this study and all surgery preparations and instrumentations were performed under clean but not aseptic conditions. Food was withdrawn ~16 hours prior to surgery, with ad-libitum access to water.

Preterm lambs. Pregnant ewes were administered intramuscular betamethasone (12 mg; Celestone, Merck Sharp & Dohme, Australia) 48 and 24 hours prior to caesarean section at 126–128 days of gestational age to deliver the preterm lambs. General anaesthesia was induced via maternal intravenous injection of 5% sodium thiopentone (20 mg/kg; Pentothal). The ewe was intubated, placed in a prone position and anaesthesia was maintained via inhaled 1–2.5% isoflurane with mechanical ventilation and fractional inspired oxygen to keep peripheral arterial oxygen saturation (SpO_2) >95%. Preterm lambs were partially exteriorized via a maternal midline abdominal incision and hysterotomy for fetal instrumentation as described previously,[21] whilst maintaining the placental-umbilical circulation. Briefly, a nonocclusive polyvinyl catheter was inserted into the fetal right carotid artery with the catheter tip at the level of the mandibular angle, before the carotid bifurcation, for administration of iodine contrast agent. The fetal left median nerve was exposed at the cubital fossa of the forelimb and a small silicon cuff containing two multi-stranded copper wire electrodes approximately 1 cm apart was placed around the median nerve.[25] The fetal lamb was then intubated (size 4.0 endotracheal tube) and lung liquid passively drained for 2 mins. The lamb was then fully exteriorized from the uterus onto the maternal abdomen, with the umbilical cord still attached and functioning, for positive pressure ventilation with humidified air in volume-guaranteed mode at tidal volumes of ~5 ml/kg using a (Babylog8000+, Draeger; Germany). Surfactant was administered via the endotracheal tube (100 mg/kg Curosurf; ChiesiPharma; Italy) after 1 min of ventilation. Delayed cord clamping was achieved with the umbilical cord clamped and cut after a total of 3 min of ventilation. The preterm lamb was then transferred to a robot-operated surgical trolley in the Optics hutch 3B of the IMBL and mechanical ventilation continued. General anaesthesia was maintained with 1 – 1.5% inhaled isoflurane. An oxygen saturation probe was placed around the lamb's shaved right forelimb to measure SpO_2 (Radical 4, Masimo, French's Forest NSW, Australia). Single-lumen catheters (5 Fr, 1270.05 polyurethane catheter, Vygon, Paris; France) were inserted into the umbilical artery for continuous measurement of mean arterial blood pressure (MABP), heart rate (HR) (DTX Plus Transducer; Becton Dickinson) and blood gas sampling (pH, PaO_2, $PaCO_2$, lactate; ABL30; Radiometer, Copenhagen, Denmark); and into the umbilical vein for fluid maintenance (10% glucose at 3 ml/kg/h).

Seven-to-ten-day old term lambs. Lambs at 7–10 days of age were induced for general anaesthesia using inhaled 4–5% isoflurane via facemask. The lamb was then intubated (size 5.0 endotracheal tube), and general anaesthesia was maintained by inhaled 1–1.5% isoflurane with mechanical ventilation. Instrumentation of the 7–10-day old term lambs with carotid arterial catheter and left median nerve stimulation cuff was the same as preterm lambs (described above). However instead of umbilical vessel catheterization, the 7–10-day old term lamb's left femoral artery was catheterized for MABP, HR and blood gas sampling, and the left femoral vein was catheterized for administration of 10% glucose (at 3 ml/kg/h) for fluid maintenance. Similar to the preterm lamb, the 7–10-day old term lamb was transferred to the IMBL and mechanical ventilation continued with minimal isoflurane anaesthesia.

Near infrared spectroscopy (NIRS)

The light emitters and detector optodes of a two-channel tissue oxygenation probe (NIRO-200, Hamamatsu Photonics, Japan) were placed bilaterally on the shaved scalp of the lamb, over the somatosensory cortex.[24,25] Measurement of changes in ΔoxyHb, ΔdeoxyHb and total haemoglobin (Δtotal Hb = ΔoxyHb+ ΔdeoxyHb) (μM.cm) in both hemispheres were recorded continuously.

Experimental protocol and data recording

All physiological recordings (MABP, HR, NIRS outputs (Δtotal Hb, ΔoxyHb, ΔdeoxyHb)) were digitally acquired continuously at a sampling rate of 1000 Hz (Powerlab; ADInstruments, Castle Hill, NSW, Australia) and recorded using LabChart 8 (ADInstruments).

The copper wire electrodes placed around the left median nerve were connected to an isolated constant-current electrical pulse generator (ISOLATOR-11 stimulator isolation unit; Axon Instruments Inc., Foster City, CA, USA) that delivered pre-programmed trains of 2 msec pulses generated by the LabChart 8 software. The amplitude of the stimulus for each

lamb was set to the minimum required to evoke a just-visible twitch of the left forelimb (usually 2–5 mA).

To elicit and record a cerebral haemodynamic response in the contralateral cortex in each animal, the median nerve was stimulated with a train of 2-msec electrical pulses at a repetition rate of 3.3 Hz.[16,21] In preterm lambs, stimulus trains of short (1.8 secs), medium (4.8 secs), or long (7.8 sec) durations were conducted, while 7–10-day old term lambs were subjected to only 4.8 and 7.8 sec stimulus trains as we have previously reported that the responses to 1.8 sec stimulation were minimal or absent in 7–10-day old term lambs.[24] The beginning of each stimulus train triggered the recording of all physiological signals over a 60-sec window, always preceded by 5 sec of pre-stimulus recording which was used as the baseline to determine the relative magnitude of change of the NIRS signals, MABP and HR following median nerve stimulation.

Fifteen repeats of each stimulus train were conducted at intervals of 66 sec, and a signal-averaged output of physiological signals (MABP, HR and NIRS) was calculated using Scope software (ADInstruments, Australia). The stimulus train durations (1.8, 4.8 and 7.8 sec) were delivered in random order in all lambs. A rest period of 15 min was allowed between stimulus trains of different durations.

Synchrotron radiation microangiography

SR cerebral microangiography in the lambs was performed as previously described.[21] In brief, the lamb was put in the prone position, facing and in line with the horizontal path of the X-ray beam. The lamb's head was then rotated anti-clockwise in the horizontal plane with the nose pointing at the 10–11 o'clock position (Figure 1(a)). This position allows optimal imaging of the right cerebral fronto-parietal hemisphere which encompasses the somatosensory cortex (contralateral to the left median nerve stimulation), as the iodine contrast was injected into the right carotid artery (Figure 1(b)).

SR microangiography was performed with monochromatic X-rays at 34 keV, above the iodine absorption K-edge energy (33.17 keV), for maximal contrast. A flux of 6×10^{11} photons/mm^2/s passed through the lamb's head and were recorded intermittently for brief periods on the Ruby X-ray detector (50 mm Nikon 1:1.4 lens). A bolus (1 ml/kg) of iodinated contrast medium (320 mg iodine/ml; Visipaque, GE Healthcare, with 20 U/kg heparin) was administered via the non-occlusive catheter in the right carotid artery at 10–20 mL/min using a syringe pump (PHD22/2000; Harvard Apparatus, Holliston, MA). High resolution cine images with 2560 x 1258pixel format were recorded at 16 frames per second at 16-bit resolution and stored in a digital frame memory system. Image acquisition was initiated immediately before injection of the iodine contrast agent, and for each angiography scan, ~1000 frames were recorded with continuous x-ray exposure (62.5 msec/frame, shutter open time). The input field (field of view) of the X-ray detector was 24 mm × 13 mm with a pixel size equivalent to 29.6 μm.

The SR cerebral microangiography was performed at baseline (prior to median nerve stimulations). The time taken for the iodine contrast agent to travel through the arterial phase and appear in transition to the capillary and venous compartments was noted. Median nerve stimulation (with 15 repeats of the stimulus train) was then performed with the physiological recording (NIRS measurements, MABP and HR). The time taken for the ΔoxyHb in the contralateral cortex (Table 2) to reach its peak/nadir following the nerve stimulation was recorded. SR microangiography was then performed during one of the repeats of the stimulus train, with the iodine contrast bolus injection timed manually so that the contrast transit time to end of arterial phase on the angiogram coincided with the time for peak/nadir ΔoxyHb response following the nerve stimulation. This optimises the microvessel visualisation at the peak of the haemodynamic functional response. Notably, due to the SR radiation creating an electric current that damages the NIRS optodes, the optodes were removed temporarily and NIRS measurements ceased during the angiography scan.

At the end of experiment, the lambs were euthanised by intravenous injection of pentobarbital at 100 mg/kg.

Image analysis (vessel counts and vessel lumen diameter measurements)

Analysis of vessel counts and vessel diameter measurements were performed as described previously.[21] Briefly, image analysis was performed using ImageJ software (version 2.0.0-rc-69/1.52p, National Institutes of Health). Images were processed by first enhancing image contrast achieved using temporal subtraction. Flat-field correction was achieved by subtracting an averaged summation of 5 consecutive frames taken prior to contrast injection from each raw image taken after injection, to remove superimposed background. Images were then median filtered (2-pixel radius) for clarity.

Five frames from each processed cine-angiogram sequence (~0.5 sec apart) recorded at the end of arterial phase were selected, before iodine contrast agent transited into the capillary and venous compartments, for image vessel counts and vessel diameter measurements (Figure 1(f)). Vessel counts were categorised according

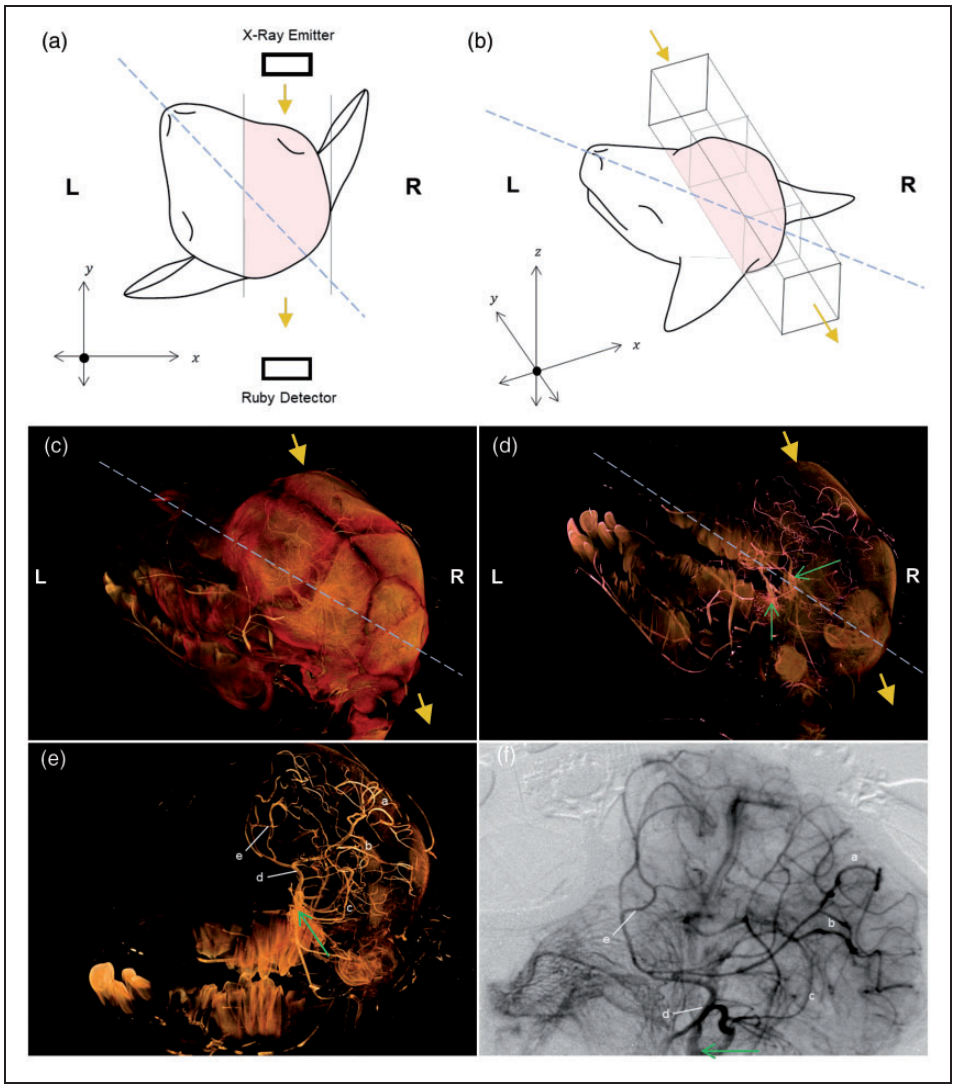

Figure 1. Correlation between the 3D anatomical vessel visualisation derived from microCT and the 2D microangiography in the right hemisphere of a preterm lamb. In figure panels A-D, blue dashed line indicates the sagittal plan and yellow arrows indicate the direction of synchrotron radiation beam utilised during 2D angiography. (a) Schematic diagram showing the 2D view (x–y plane) from above, with the sagittal line of the lamb's head pointing at the 10–11 o'clock position and the synchrotron radiation beam in the direction of the y-axis (yellow arrow). Solid lines denote the boundaries of the field-of-view (pink shaded region). (b) Schematic diagram showing the 3D view of the region of interest imaged by the synchrotron radiation (pink shaded region). Note that the lamb head position corresponds with that in the microCT images in panels (c and d). (c). MicroCT volume (with the lamb head position same as in panel B) illustrating the right hemisphere imaged by the synchrotron radiation beam (yellow arrows) in relation to the sagittal plane. (d). MicroCT cerebral vascular cast in relation to surrounding cranium (as seen in panel C, now semi-opaque). Green arrows indicate the left and right internal carotid artery. The vessels in the right cerebral hemisphere are imaged by the synchrotron radiation beam, as illustrated in panel (b). (e) The cranium is now transparent and left cerebral hemisphere is digitally removed to reveal barium filled vessels in the right cerebral hemisphere, corresponding with vessels identified on the 2D angiography (panel F). Letters a to e indicate landmark vessels across right cerebrum seen in both panels (e) and (f). (f) In vivo dynamic angiogram recorded from the same lamb following temporal subtraction (see methods for details) where black vessels indicate radiopaque iodine contrast agent filled arterial vessels. Contrast agent delivery was made through a catheter placed in the right internal carotid artery (green arrow).

to vessel lumen diameter (0–200, 201–400, 401–600, 601–800, >800 μm) in each lamb.

Vessel internal diameter measurements were performed on ImageJ and corrected for pixel size (1 pixel = 29.6 μm). Three measurements of each vessel were taken and averaged in each frame, then the averaged vessel diameter across all 5 frames was calculated, at baseline and following each stimulation

duration. The spatial point of measurement was consistent across baseline and stimulation images for each animal to calculate percentage change in vessel diameter from baseline. Vessels were classified into vessel size classes (0–200 μm, 201–500 μm, >500 μm) according to their internal diameters at baseline (Figure 3).

Ex vivo micro-computed tomography (micro-CT) with 3D volume reconstruction

To verify location of the vessels visualised on the 2D microangiography, ex-vivo micro-CT with 3D reconstruction of the cerebral vasculature was performed in a preterm lamb. Following euthanasia, barium sulfate contrast (20% w/v, gelatine 5% w/v) was infused into the cerebral circulation via the right carotid artery catheter. The lamb neck was tied distally to the right carotid artery to prevent efflux of barium and allow the barium to firm. The lamb head was then removed and fixed in 10% formalin.

The CT scans were conducted at IMBL, using 33.8 keV X-ray photon energy and the facility's Ruby detector (50 mm lens, 20 μm phosphor scintillator) with a 2.5 m sample-to-detector distance. The X-ray system was tuned to produce 2D images for a field of view of 75 × 36 mm with 29.6 μm pixel size. CT data acquisition for the lamb head consisted of 3 overlapping scans, each containing 1800 projections over a 180° axis. Multiple scans were required to accommodate the full image of the head. The exposure was 55 msec per projection with an accumulated time of ~5 mins to scan the lamb head. Each image projection was then processed to subtract electronic noise and background by subtracting the median of 50 background and 50 dark-field images taken without the sample (the lamb head). Reconstruction of a 3D rendered series of CT cross-sectional slices, including cropping, stitching and flat field subtraction, was performed using the CTAS package (https://github.com/antonmx/ctas), and the pre-processed data were then piped into the CSIRO's Xtract software[27]) to perform actual CT computation. The results were post-processed (noise reduction, downsizing, 8-bit conversion) in Fiji (https://imagej.net/Fiji). These steps were automated using custom IMBLproc scripts and user interfaces (https://github.com/AustralianSynchrotron/imblproc). Reconstructed slices were stored as 8-bit TIFF volumetric images. Three dimensional visualisation and manipulation of the lamb head, including digital removal of tissue layers, i.e. skin and cranium to reveal the vasculature, was performed using Drishti (version 2.6, github.com/AjayLimaye/drishti) (Figure 1(c) to (e)). The 3D micro-CT cerebral vascular cast confirms that vessels in the right somatosensory cortex were imaged in the *in vivo* 2D microangiograms (Figure 1(d) to (f)).

Physiological data analyses

The MABP and NIRS data from the 60-sec post-stimulus window of recording were averaged as consecutive 1-sec duration bins and expressed as changes from the pre-stimulus baseline.

Analysis and classification of the NIRS response patterns in the contralateral cortex (the right hemisphere) were based on ΔoxyHb, as it presents a more robust signal-to-noise ratio than ΔdeoxyHb as reported previously by us[16] and elsewhere.[28] A 'positive' or 'negative' response was defined as an increase or decrease of oxyHb in the contralateral hemisphere, of more than 2 standard deviations from the baseline data values recorded over 5 sec immediately before the onset of the median nerve stimulation.

Statistical analyses

Statistical analyses were performed using SigmaPlot 14.5 (Systat Software) and GraphPad Prism 7 (GraphPad Software, La Jolla; USA). Normality was assessed by the Shapiro-Wilk test. Physiological parameters and arterial blood gas measurements were compared between those at the start and the end of the experiment, using the Student's paired t-test for parametric data or Wilcoxon signed-rank test for non-parametric data. For cerebral vessel numbers and percentage change in vessel diameter, one way repeated measures ANOVA was used to compare between durations of stimulations and between vessel diameter categories with Tukey's post hoc analysis, whereas the differences between preterm and 7–10-day old term lambs were compared using a Welch's t-test which does not assume equal variance in the 2 groups. Effects of the 3 durations of stimulation on MABP and NIRS parameters in the preterm lambs were compared using one-way repeated measures ANOVA, with Tukey's post hoc analysis for parametric data and Friedman test for non-parametric data. All results are expressed as mean ± SD, and P value <0.05 was considered significant.

Results

Preterm and 7–10-day old term lamb characteristics

Seven preterm lambs and four 7–10-day old term lambs were subjected to general anaesthesia and mechanical ventilation for 4–5 h. There were no significant differences in weight, arterial blood gas parameters or heart rate between the start and end of the experiment in both preterm and 7–10-day old term lambs (Supplementary Table 1). Blood pressure decreased in preterm lambs between the start and end of the

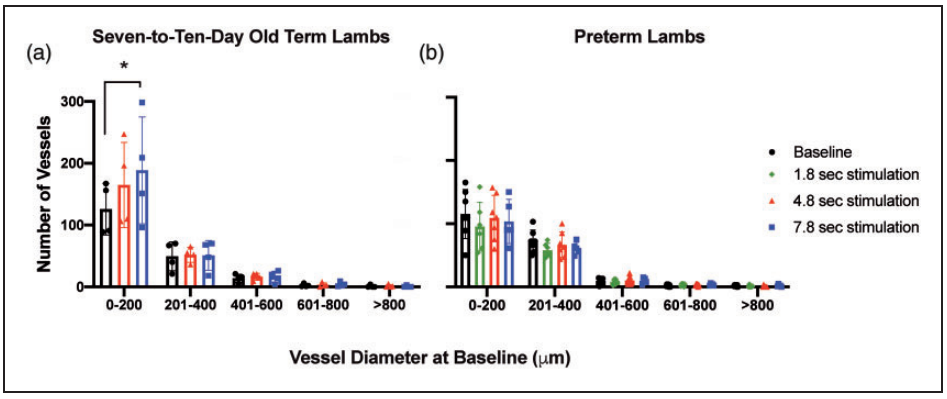

Figure 2. Cerebral vessel counts.
Number of microvessels categorised according to vessel diameters in (A) 7–10-day old term (n = 4) and (B) preterm lambs (n = 7) at baseline (black) and following 1.8 sec (green), 4.8 sec (red) and 7.8 sec (blue) stimulation. Seven-to-ten-day old term lambs were subjected to 4.8 and 7.8 sec stimulus trains and preterm lambs to 1.8, 4.8 and 7.8 sec stimulus trains. Values are shown as mean ± SD. *$p < 0.05$ between vessel counts with different stimulation durations.

experiment, however it remained within the normal physiological range under these experimental conditions.[29]

Using 3D microCT to localise the vessels seen on 2D SR microangiography

A preterm lamb's head was prepared for 3D microCT imaging in order to verify locations of the vessels seen on the 2D SR microangiography. An example is shown in Figure 1. The brain region imaged by the 2D SR microangiography is shown schematically in Figure 1 (a) and (b). The microCT of the lamb head (Figure 1 (c)) allowed 3D anatomical visualization of the blood vessels in the right cerebral hemisphere of the lamb, as seen after digitally removing the cranium (Figure 1(d)) and the left cerebral hemisphere (Figure 1(e)). Landmark vessels identified on the *in vivo* 2D SR microangiography could be correlated with the vessels seen on the 3D microCT image in the right somatosensory cortex (Figure 1(e) and (f)), confirming that appropriate regional vessels were used for analyses on the SR angiography after left-sided somatosensory nerve stimulations.

Changes in number of cerebral vessels following somatosensory stimulation

SR cerebral microangiography was obtained in all 7–10-day old term lambs following stimulus trains of 4.8 and 7.8 sec durations. In preterm lambs, SR microangiography was obtained in 6/7 lambs following 1.8 sec stimulations, in 7/7 lambs following 4.8 sec stimulation and 5/7 lambs following 7.8 sec stimulation. The number of cerebral microvessels visible in angiography images were counted, categorised according to vessel diameters, and compared between baseline (before median nerve stimulations) and following the nerve stimulations (Figure 2).

Seven-to-ten-day old term lambs (Figure 2(a)): The number of the small microvessels (≤200 μm diameter) following 7.8 sec stimulations was increased to 188.5 ± 86.4 compared to baseline (125.8 ± 41.5, $p < 0.05$). There was no change in the number of vessels of larger diameters (>200 μm) after the median nerve stimulations.

At baseline and following median nerve stimulation for 7.8 sec, the number of vessels of ≤200 μm in diameter was significantly greater compared to vessel categories of diameters >800 μm ($p < 0.05$). Following 4.8 sec stimulation, the number of vessels with a diameter ≤200 μm was significantly greater compared to vessel of diameters 601–800 μm and >800 μm ($p < 0.05$).

Preterm Lambs (Figure 2(b)): There was no significant change in the number of vessels in any vessel diameter categories after stimulation for any of the 1.8, 4.8 or 7.8 sec durations, compared to the baseline. At baseline, and following 1.8, 4.8 and 7.8 sec stimulations respectively, the number of the smallest microvessels (≤200 μm diameter) were significantly greater than the number of vessels with diameters between 601–800 μm and >800 μm ($p < 0.05$).

Change in diameter of cerebral vessels

The relative (percentage) changes in the internal diameter of cerebral vessels in the contralateral somatosensory cortex following median nerve stimulations were categorised according to their baseline diameters and averaged for each lamb (Figure 3). Cerebral vessels as

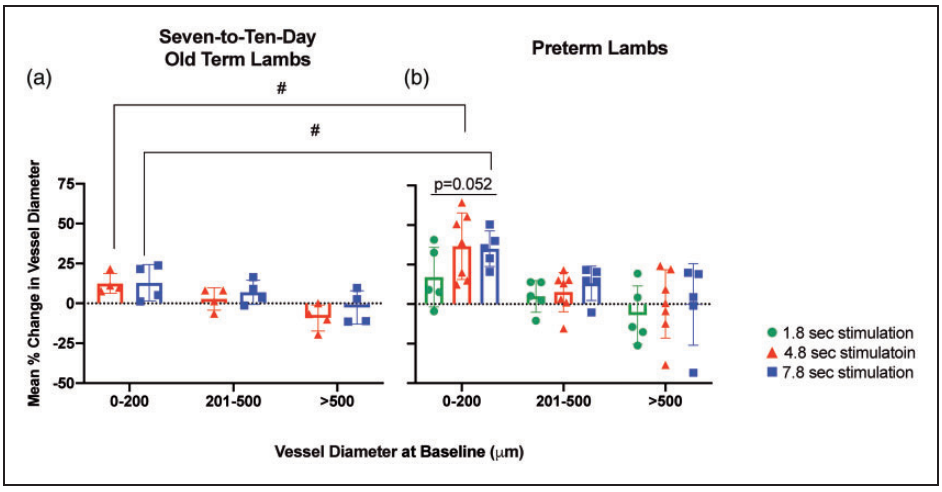

Figure 3. Categorised vessel diameter change of lambs following median nerve stimulation. Percentage change of vessel diameters of (A) 7–10-day old term lambs (n = 4) following 4.8 sec (red) and 7.8 sec (blue) stimulations; (B) preterm lambs (n = 7) following 1.8 sec (green), 4.8 sec (red) and 7.8 sec (blue) stimulations. Values are shown as mean ± SD. #$p < 0.05$ between 7–10-day old term and preterm lambs at the same stimulation duration.

small as ~90 μm diameter could be visualised and measured.

Seven-to-ten-day old term lambs *(Figure 3(a))*. There were no significant differences in the diameter changes between the 4.8 sec and 7.8 sec stimulations within any vessel diameter category. Following 4.8 sec and 7.8 sec stimulations respectively, percentage changes in diameter of the smallest vessels (≤200 μm) were significantly greater compared to changes in the largest vessels (>500 μm) ($p < 0.05$).

Preterm lambs *(Figure 3(b))*. Cerebral microvessels with diameters ≤200 μm showed increased vessel diameters following all stimulation durations. There was a strong trend for higher percentage increase in vessel diameter following the longer stimulation durations of 4.8 and 7.8 sec (36.6 ± 21.0% and 35.0 ± 11.3% respectively), compared to the 1.8 sec stimulation (17.1 ± 18.9%, $p = 0.052$). No difference in percentage diameter changes was seen between the 3 stimulation durations in vessels of larger diameters (>200 μm).

Following median nerve stimulations of 1.8, 4.8 and 7.8 sec respectively, the percentage increase in the diameter of the smallest vessels (≤200 μm diameter) was significantly greater compared to vessels with diameters >500 μm ($p < 0.05$).

Comparison between preterm and 7–10-day old term lambs. Compared to 7–10-day old term lambs, the preterm lambs showed significantly higher percentage increases in vessel diameters of microvessels with diameters ≤200 μm during 4.8 and 7.8 sec stimulations respectively (Figure 3, $p < 0.05$).

NIRS measurement of cerebral haemodynamic responses to somatosensory stimulation

Table 1 summarises the incidence, and Table 2 summarises the amplitude and timing of the cerebral haemodynamic response patterns measured by NIRS following different stimulation durations, based on changes in ΔoxyHb signal in the contralateral cortex. NIRS data could not be obtained for 1 seven-to-ten-day old term lamb and 1 preterm lamb due to technical difficulties (Table 1).

One out of 3 seven-to-ten-day old term lambs had a positive (increased) ΔoxyHb response and 2 lambs had a negative (decreased) ΔoxyHb response following 4.8 sec stimulations. However, 2 out of 3 seven-to-ten-day old term lambs had a positive ΔoxyHb response and 1 lamb had a negative ΔoxyHb response following 7.8 sec stimulations (Table 1, Figure 4(a), (c), (e), (g)). All preterm lambs had a positive ΔoxyHb response following 1.8, 4.8 and 7.8 sec stimulations (Table 1, Figure 4(b), (d), (f), (h)). These observations are consistent with our previous studies demonstrating that somatosensory stimulation evokes variable responses in 7–10-day old term lambs[24] and mostly positive cerebral hemodynamic responses in preterm lambs.[25]

Changes in blood pressure and cerebral ΔHb after somatosensory stimulation (Table 2)

Mean arterial blood pressure. Combining the 7–10-day old term lambs with positive and negative responses,

Table 1. Contralateral ΔoxyHb response pattern in preterm and 7–10-day old term lambs.

		Contralateral ΔoxyHb response pattern			
	Duration of stimulation	No. of lambs studied (n)	Positive (n)	Negative (n)	NIRS recording not available (n)
Seven-to-ten-day old term lambs	4.8 sec	4	1	2	1
	7.8 sec	4	2	1	1
Preterm lambs	1.8 sec	6	5	0	1
	4.8 sec	7	6	0	1
	7.8 sec	5	4	0	1

Note: Incidence of positive, negative or no response pattern, based on changes in oxyhaemoglobin (ΔoxyHb) recorded by NIRS from the contralateral hemisphere, in 7–10-day old term lambs following median nerve stimulation at 3.3 Hz for 4.8 or 7.8 sec and preterm lambs following median nerve stimulation at 3.3 Hz for 1.8, 4.8 or 7.8 sec.

Table 2. Changes in physiological parameters in preterm and 7–10-day old term lambs.

		1.8 sec		4.8 sec		7.8 sec	
Seven-to-ten-day old term lambs (n = 4)		–	–	Positive (n = 1)	Negative (n = 2)	Positive (n = 2)	Negative (n = 1)
ΔMABP	Time to peak (sec)	–	–	8	8, 8	10, 10	29
	Peak amplitude (mmHg)	–	–	0.9	1.0, 0.7	3.1, 2.69	0.4
Contralateral	Time to peak/nadir (sec)	–	–	9	13, 14	12, 7	15
ΔoxyHb	Peak amplitude (μM.cm)	–	–	5.4	–11.5, –6.2	7.9, 7.0	–4.2
Preterm Lambs (n = 7)		Positive (n = 5)	Negative (n = 0)	Positive (n = 6)	Negative (n = 0)	Positive (n = 4)	Negative (n = 0)
ΔMABP	Time to peak (sec)	6.2 ± 1.6	–	8 ± 0.6	–	11.3 ± 1.0*	–
	Peak amplitude (mmHg)	3.5 ± 2.6	–	5.9 ± 3.9	–	4.1 ± 1.3	–
ContralateralΔoxyHb	Time to peak/nadir (sec)	10.8 ± 2.8	–	12.3 ± 6.9	–	13.8 ± 1.9	–
	Peak amplitude (μM.cm)	6.6 ± 2.9	–	9.3 ± 11.4	–	7.8 ± 4.0	–

Note: Changes in physiological parameters in preterm lambs with positive or negative contralateral ΔoxyHb response, following median nerve stimulation for 4.8 sec and 7.8 sec in 7–10-day old term lambs and 1.8 sec, 4.8 sec and 7.8 sec in preterm lambs (values are mean ± SD; individual values are shown where $n < 3$ available). Values are shown as mean ± SD. * indicates significant difference between 7.8 sec and 4.8 sec ($p < 0.05$).

there is no difference in their mean peak ΔMABP compared to that in preterm lambs following 4.8 or 7.8 sec stimulations. In 7–10-day old term lambs, the peak ΔMABP following stimulation and the times taken to reach the peak MABP were similar in all lambs following 4.8 sec and 7.8 sec stimulations, except the 1 lamb with a negative ΔoxyHb response after 7.8 sec stimulation which responded with a delayed and minimal change in MABP.

In preterm lambs, the time taken to reach peak MABP was significantly greater following 7.8 sec compared to 4.8 sec stimulations ($p < 0.05$). No significant differences in peak ΔMABP were seen between different stimulation durations in preterm lambs.

Cerebral OxyHb. The amplitudes of or time to reach the peak ΔoxyHb were similar between preterm and 7–10-day old term lambs with positive responses. In preterm lambs, there were no significant differences between the 3 stimulation durations in the amplitude of or time to reach peak ΔoxyHb.

Cerebral vessel dilation and constriction

A representative example of the SR microangiography is shown in Figure 5 illustrating that cerebral vessels in different areas can show dilation or constriction during a 7.8 sec stimulation. The NIRS optode placed over the somatosensory cortex recorded increased ΔoxyHb (positive response) with the stimulation, corresponding to some of the dilated vessels near the optode (Figure 5; green circles).

Discussion

We have previously utilised synchrotron microangiography to investigate cerebral haemodynamics in the preterm newborn lamb which has a brain size comparable to that of the human newborn.[21] The current study has explored and extended the use of synchrotron

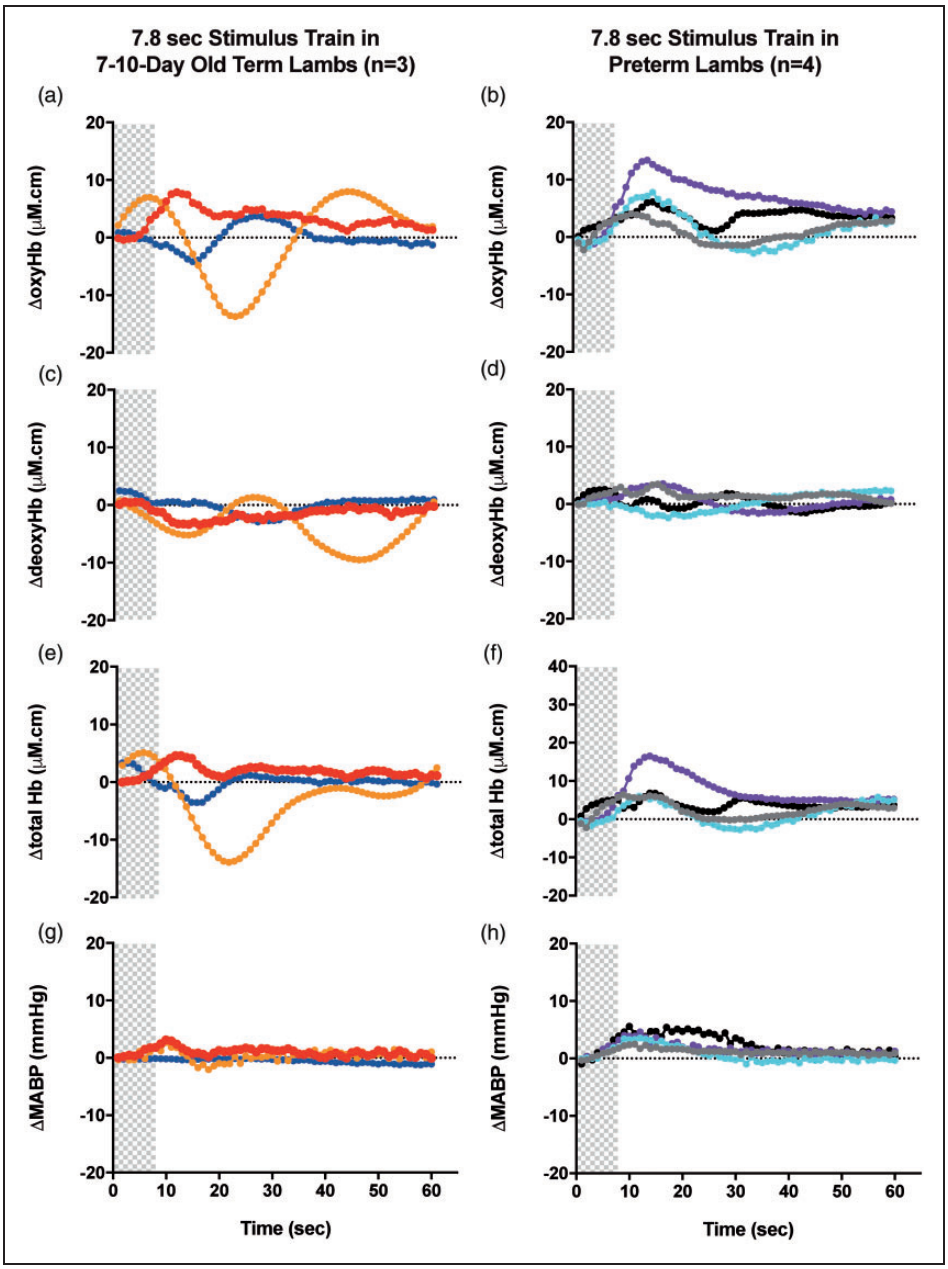

Figure 4. Changes in oxy-, deoxy- and total haemoglobin (ΔoxyHb; A, B, ΔdeoxyHb; C, D and Δtotal Hb; E,F) recorded from the contralateral hemispheres, and mean arterial blood pressure (ΔMABP; G,H), following a 3.3 Hz stimulus train of 7.8 sec duration in 7–10-day old term (A, C, E, G) and preterm lambs (B, D, F, H). Individual lambs are shown by different colours. Shaded area in each graph shows the period of stimulation.

microangiography in functional brain imaging for the first time and has characterised the functional haemodynamic response based on changes in microvessels in the immature brain. We found that in response to somatosensory stimulation of increasing durations in the 7–10-day old term lambs, more cerebral microvessels were recruited as indicated by vessel contrast transit and visualisation, but there was no overall change in the vessel diameters of the visibly perfused vessels at different durations of stimulation. In contrast, the preterm brain responded to increasing durations of neural stimulations with further dilatation of the cerebral microvessels (i.e., increasing vessel diameter). Importantly, these increases in vessel diameter in preterm lambs occur without the recruitment of additional vessels. Our findings suggest different vascular mechanisms underly the cerebrovascular response in the 7–10-day old brain vs. preterm brain.

Functional imaging studies of the development of the cerebrovascular response from early postnatal life

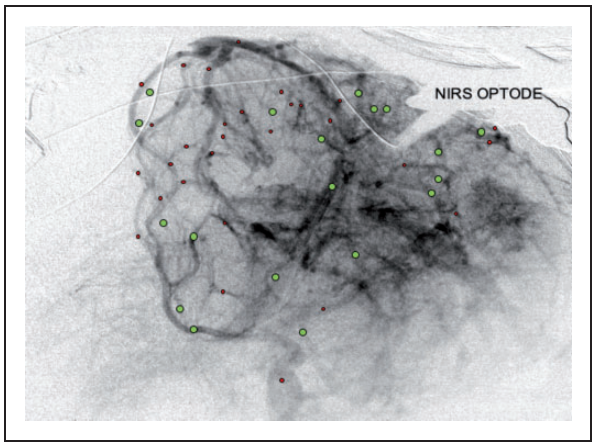

Figure 5. Cerebral vessels dilatation and constriction in a representative image of cerebral micro-angiography with iodine contrast injected via the right carotid arterial catheter. The NIRS optodes on the right parietal region could be seen. Cerebral vessels are schematically indicated to show those with increased diameter (vasodilation, green) or decreased diameter (vasoconstriction, red) during a 7.8 sec stimulation. Vessels shown are those that consistently displayed clear contrast entry and vessel wall in all 5 image frames used for analysis at baseline and during the stimulation.

have reported dramatically different developmental trajectories that fall into two broad categories: (i) a positive response (i.e., a localised increase in oxyHb and/or decrease in deoxyHb, or a positive BOLD fMRI signal) which increases in amplitude and decreases in latency from newborn to adults[6,30]; or (ii) a negative response (localised decrease in oxyHb and/or increase in deoxyHb) in early postnatal life, which then switches to a positive response at a later age.[7,10–12] Mechanisms that underlie these developmental changes in the neurovascular coupling response from newborn to adulthood is unclear, but is likely due to the maturation and development of key components of the neurovascular unit.[6]

Between the preterm and 7–10-day old term lambs, we did not identify any differences in the peak amplitude or latency of the positive ΔoxyHb response in this current cohort or our published data of newborn lambs.[24,25] Nevertheless, our current SR findings suggest the underlying vascular mechanisms are evidently different between the 7–10-day old term brain and preterm brain.

Interestingly, studies in newborn rodents failed to record a BOLD fMRI signal prior to postnatal day 13 of age,[6] suggesting that the functional cerebrovascular response develops with maturation. Notably, the rodent brain development at postnatal age of 7–10 days is considered comparable to the term human infant in terms of glial, vascular and synaptic growth.[31] Several processes which occur around this age may underlie the appearance of a measurable cerebral haemodynamic response in human-term-equivalent rodent brain. These include vascular sprouting around postnatal day 10 and the development of arterial or venous characteristics; a rise in CBF to near-adult levels; astrocyte proliferation (which do not mature in rats until ~day 21) and its gap-junction coupling[32,33]; increased synthesis of prostanoids in the brain; synaptogenesis with development of sensory stimulus–evoked potentials; and increased sensitivity of the cerebral microcirculation to vasoactive stimuli.[6] In the human fetal cortex, microvasculature develops radially from the superficial leptomeningeal vessels, with muscularization of the extra-striatal arterioles and capillary beds not established until close to term equivalent age.[34,35] All these factors are likely also vital to the ability to 'recruit' or open up additional cerebral microvessels following neural stimulations, which may explain our observations in the 7–10-day old term lamb brain compared to preterm lambs. The increased recruitment of cerebral vessels may also underlie the higher amplitude and shorter latency of the cerebral haemodynamic response with increasing age, as reported in humans and rats.[6,30]

The increase in MABP following somatosensory stimulation is likely to be due to activation of the sympathetic nervous system from recruitment of segmental spinal reflexes, which is associated with involvement of the ascending nociceptive pathways.[36] We previously have reported no correlation between the cerebral ΔoxyHb and ΔMABP in larger cohorts of fetal[16] and newborn preterm lambs[25] at the same gestational age and exposed to the same experimental protocol as in the current study, suggesting that the cerebral haemodynamic response is not driven by the increase in MABP.

Despite the increased number of visible cerebral vessels, NIRS measurements in some 7–10-day old term lambs showed the negative response with decreased ΔoxyHb, consistent with our published data[24] and is suggestive of local arterial vasoconstriction as observed in neonatal rodents[10,11] and human neonates.[12] This vasoconstriction phase was proposed to be driven by innervation of the cerebral vessels[37] and was also observed in the adult rat[10] where it was proposed that it served to return hyperaemia to baseline. Accordingly, this vasoconstriction may also cause CBF to decrease below the basal (normal) level of perfusion in brain tissue surrounding the responding region, potentially explaining the 'vascular steal' reported in other studies.[38,39] We also noted regional differences in the cerebral haemodynamics on the SR microangiography (Figure 5).

Utility of SR microangiography

A variety of techniques have been developed for functional neuroimaging in both human and animal studies

to investigate the cerebral response to neural activity, including different MR techniques, positron emission tomography (PET), magnetoencephalography/magnetic source imaging, transcranial doppler ultrasound and NIRS, or local brain tissue $_{P}O_{2}$.[40] Many of these techniques rely on measuring the haemodynamic responses as indicated by the changes in cerebral oxy and deoxyhaemoglobin, rather than the actual vascular changes. Optical coherence tomography[41] and ultrafast ultrasound localization microscopy[42] mostly apply to small rodent brains due to the limited imaging depth (<10 mm).

Our study demonstrates the utility of SR microangiography in direct measurements of the intraparenchymal cerebral vasculature, which has previously been difficult due to methodological constraints. Transcranial Doppler measures blood flow velocity of main cerebral arteries in human studies, but not regional intraparenchymal changes. Similarly, studies of newborn rodents use optical spectral imaging to directly measure calibres of upstream vessels on the cortical surface (e.g., pial arterioles),[10] or use laser Doppler placed on the cortical surface to measure the upstream CBF.[11] While the pial circulation is responsible for a sizable fraction of the total resistance (and hence, with a potential for flow control), a larger component of the overall resistance is attributable to downstream intracerebral vessels.[43] We have previously shown in newborn lambs that the neurovascular coupling response may differ between upstream and downstream vessels, such that even when the superficial cortical blood flow (measured by laser Doppler) increases in response to somatosensory stimulation, the intraparenchymal response measured by NIRS could show reduced total- and oxy-Hb, indicating the importance of downstream vasoconstriction.[24] Indeed, there is also emerging evidence of functional segmentation of the cerebrovascular tree in various cortical regions, with gradual phenotypic change (zonation) and different signalling mechanisms responsible for vasodilation along the continuum of the arteriovenous network.[44,45] There is also structural diversity of the neurovascular unit along the cerebrovascular tree suggesting differences in the role of each vascular segment in the overall regulation of CBF. For example, pial arterioles have multiple layers of smooth muscle cells and are richly innervated, while the intraparenchymal arterioles have a single or discontinuous layer of smooth muscle cells, lack perivascular nerves and are encased by astrocytic end-feet.[46] Nevertheless, the different signalling mechanisms responsible for vasodilation at different levels of the cerebrovascular tree are not yet fully understood.[45,46]

To address some of these issues, we used SR angiography to directly measure intraparenchymal vessels. We use the preterm sheep model as it offers significant advantages in studying cerebrovascular development due to its similarities to the human neonatal brain in size, structure and cerebrovascular reactivity.[23] While SR microangiography can detect dynamic intraparenchymal microvascular changes in the lamb brain, the method has several limitations. The images are two-dimensional and require contrast administration. We also had to balance between the compromise of spatial resolution and size of the field-of-view for the microangiograms. To achieve higher resolution with a smaller pixel size for measuring smaller microvessels, the field of view would have to be reduced in size and restricted to a smaller brain region. This could result in an inability to capture the vessels of interest, especially given the overall size of the lamb brain. Our post-mortem 3D microCT (Figure 1) confirmed that with our selected spatial resolution and size of field-of-view, the SR microangiography clearly captured the cerebral microvessels within our region of interest (the contralateral somatosensory cortex). Using images selected at the end of the arterial phase before the iodine contrast transited to the capillary and venous compartments, the vessels we analysed were small arteries and arterioles (capillaries are not visible on the microangiogram except as a "blush"). However, we are unable to reliably differentiate between small arteries and arterioles. Also, while our study has described the vascular changes, further studies are clearly required to investigate the mechanisms underlying the age-related changes in neurovascular responses at the cellular and molecular level.

Significance/conclusion

To our knowledge, this is the first study to use SR microangiography to characterise the cerebral haemodynamic functional response in the developing brain. Our results have revealed an important mechanistic difference between the 7–10-day old term brain and preterm brain in their cerebrovascular responses to somatosensory stimulations. In the preterm brain cerebral vessels dilate but there is no recruitment or 'opening' of minimally perfused vessels, while the 7–10-day old term brain recruits more vessels without further dilation of the vessels visible at resting condition. The lack of vessel recruitment in the preterm brain may suggest a potentially limited capacity to mount higher cerebral haemodynamic responses when faced with prolonged or stronger neural stimulations.

Neurovascular interactions have emerged as essential contributors to brain development and vital for maintaining the homeostasis of the brain internal milieu.[46] Notably, preterm brain injury is largely attributable to cerebrovascular lesions,[47] but the role of

neurovascular coupling was traditionally not considered and its pathogenic impact remains to be established. The development of cerebrovascular responses to neural stimulations may underlie important mechanisms of preterm brain injury and provide therapeutic targets. In addition, oxidative stress and inflammation, major causes of neurovascular dysfunction in adult neurological diseases,[46] are also recognised as major contributors of preterm brain injury.[48] These factors could also drive neurovascular dysfunction in the preterm brain, amplifying the pathogenic impact.

Data availability statement

The data that support the findings of this study are available from the corresponding author upon reasonable request.

Funding

The author(s) disclosed receipt of the following financial support for the research, authorship, and/or publication of this article: This study was supported by the Victorian Government's Operational Infrastructure Support Program, the In-kind Australia's Nuclear Science and Technology Organisation (ANSTO) Grant, and Fund for the Promotion of Joint International Research by Japan Society For the Promotion of Science (JSPS Number: 15KK0311); G.R. Polglase was supported by a National Health and Medical Research Council (NHMRC) and National Heart Foundation of Australia Fellowship (1105526), F.Y. Wong has been supported by NHMRC Career Development Fellowships (1084254 and 1159120).

Acknowledgements

We acknowledge the technical support provided by Dr Ilias Nitsos and Dr Mitzi Klein for the animal surgery and technical support at the animal surgery, and Dr Chris Hall for his technical assistance at the IMBL.

Declaration of conflicting interests

The author(s) declared no potential conflicts of interest with respect to the research, authorship, and/or publication of this article.

Authors' contributions

I.M. Inocencio and N.T. Tran: Collection, assembly, analysis and interpretation of data; drafting the article and revising it critically; final approval of manuscript; S.Nakamura: Conception and design of the experiments, establishment of protocols and methods, interpretation of data; critical revision of the article; final approval of manuscript; S.J. Khor, M. Wiersma and K. Stoecker: Collection, assembly, analysis and interpretation of data; critical revision of the article; final approval of manuscript; A. Maksimenko and G.R. Polglase; Conception and design of the experiments, analysis and interpretation of data; critical revision of the article; final approval of manuscript; J.T. Pearson, D.W. Walker and F.Y. Wong: Conception and design of the experiments; collection, assembly, analysis and interpretation of data; drafting the article and revising it critically; final approval of manuscript.

Supplemental material

Supplemental material for this article is available online.

References

1. Fox PT and Raichle ME. Focal physiological uncoupling of cerebral blood flow and oxidative metabolism during somatosensory stimulation in human subjects. *Proc Natl Acad Sci U S A* 1986; 83: 1140–1144.
2. Arichi T, Moraux A, Melendez A, et al. Somatosensory cortical activation identified by functional MRI in preterm and term infants. *NeuroImage* 2010; 49: 2063–2071.
3. Taga G, Asakawa K, Maki A, et al. Brain imaging in awake infants by near-infrared optical topography. *Proc Natl Acad Sci U S A* 2003; 100: 10722–10727.
4. Slater R, Cantarella A, Gallella S, et al. Cortical pain responses in human infants. *J Neurosci* 2006; 26: 3662–3666.
5. Bartocci M, Bergqvist LL, Lagercrantz H, et al. Pain activates cortical areas in the preterm newborn brain. *Pain* 2006; 122: 109–117.
6. Colonnese MT, Phillips MA, Constantine-Paton M, et al. Development of hemodynamic responses and functional connectivity in rat somatosensory cortex. *Nat Neurosci* 2008; 11: 72–79.
7. Anderson AW, Marois R, Colson ER, et al. Neonatal auditory activation detected by functional magnetic resonance imaging. *Magnetic Resonance Imaging* 2001; 19: 1–5.
8. Seghier ML, Lazeyras F, Zimine S, et al. Combination of event-related fMRI and diffusion tensor imaging in an infant with perinatal stroke. *NeuroImage* 2004; 21: 463–472.
9. Heep A, Scheef L, Jankowski J, et al. Functional magnetic resonance imaging of the sensorimotor system in preterm infants. *Pediatrics* 2009; 123: 294–300.
10. Kozberg MG, Chen BR, DeLeo SE, et al. Resolving the transition from negative to positive blood oxygen level-dependent responses in the developing brain. *Proc Natl Acad Sci USA* 2013; 110: 4380–4385.
11. Zehendner CM, Tsohataridis S, Luhmann HJ, et al. Developmental switch in neurovascular coupling in the immature rodent barrel cortex. *PLoS One* 2013; 8: e80749.
12. Kusaka T, Kawada K, Okubo K, et al. Noninvasive optical imaging in the visual cortex in young infants. *Hum Brain Mapp* 2004; 22: 122–132.
13. Hintz SR, Benaron DA, Siegel AM, et al. Bedside functional imaging of the premature infant brain during passive motor activation. *J Perinat Med* 2001; 2: 335–343.
14. Kozberg M and Hillman E. Neurovascular coupling and energy metabolism in the developing brain. *Prog Brain Res* 2016; 225: 213–242.
15. Mullinger KJ, Mayhew SD, Bagshaw AP, et al. Evidence that the negative BOLD response is neuronal in origin: a simultaneous EEG-BOLD-CBF study in humans. *NeuroImage* 2014; 94: 263–274.

16. Nakamura S, Walker DW and Wong FY. Cerebral haemodynamic response to somatosensory stimulation in near-term fetal sheep. *J Physiol* 2017; 595: 1289–1303.
17. Zhang M, Peng G, Sun D, et al. Synchrotron radiation imaging is a powerful tool to image brain microvasculature. *Med Phys* 2014; 41: 031907.
18. Liu P, Sun J, Zhao J, et al. Microvascular imaging using synchrotron radiation. *J Synchrotron Radiat* 2010; 17: 517–521.
19. Reina-De La Torre F, Rodriguez-Baeza A and Sahuquillo-Barris J. Morphological characteristics and distribution pattern of the arterial vessels in human cerebral cortex: a scanning electron microscope study. *Anat Rec* 1998; 251: 87–96.
20. Shirai M, Schwenke DO, Tsuchimochi H, et al. Synchrotron radiation imaging for advancing our understanding of cardiovascular function. *Circ Res* 2013; 112: 209–221.
21. Inocencio IM, Tran NT, Nakamura S, et al. Increased peak end-expiratory pressure in ventilated preterm lambs changes cerebral microvascular perfusion: direct synchrotron microangiography assessment. *J Appl Physiol (1985)* 2020; 129: 1075–1084.
22. Gunn AJ and Bennet L. Fetal hypoxia insults and patterns of brain injury: insights from animal models. *Clin Perinatol* 2009; 36: 579–593.
23. Back SA, Riddle A, Dean J, et al. The instrumented fetal sheep as a model of cerebral white matter injury in the premature infant. *Neurotherapeutics* 2012; 9: 359–370.
24. Nakamura S, Walker DW and Wong FY. Cerebral haemodynamic response to somatosensory stimulation in neonatal lambs. *J Physiol* 2017; 595: 6007–6021.
25. Inocencio IM, Tran NT, Khor SJ, et al. The cerebral haemodynamic response to somatosensory stimulation in preterm newborn lambs is reduced with dopamine or dobutamine infusion. *Exp Neurol* 2021; 341: 113687.
26. Percie Du Sert N, Hurst V, Ahluwalia A, et al. The ARRIVE guidelines 2.0: updated guidelines for reporting animal research. *BMJ Open Sci* 2020; 4: e100115.
27. Gureyev TE, Nesterets Y, Ternovski D, et al. Toolbox for advanced X-ray image processing. *Proc Spie* 2011. 8141.
28. Bortfeld H, Wruck E and Boas DA. Assessing infants' cortical response to speech using near-infrared spectroscopy. *NeuroImage* 2007; 34: 407–415.
29. Polglase GR, Morley CJ, Crossley KJ, et al. Positive end-expiratory pressure differentially alters pulmonary hemodynamics and oxygenation in ventilated, very premature lambs. *J Appl Physiol (1985)* 2005; 99: 1453–1461.
30. Arichi T, Fagiolo G, Varela M, et al. Development of BOLD signal hemodynamic responses in the human brain. *NeuroImage* 2012; 63: 663–673.
31. Semple BD, Blomgren K, Gimlin K, et al. Brain development in rodents and humans: identifying benchmarks of maturation and vulnerability to injury across species. *Prog Neurobiol* 2013; 106–107: 1–16.
32. Binmöller FJ and Müller CM. Postnatal development of dye-coupling among astrocytes in rat visual cortex. *Glia* 1992; 6: 127–137.
33. Muller CM. Astrocytes in cat visual cortex studied by GFAP and S-100 immunocytochemistry during postnatal development. *J Comp Neurol* 1992; 317: 309–323.
34. Norman MG and O'Kusky JR. The growth and development of microvasculature in human cerebral cortex. *J Neuropathol Exp Neurol* 1986; 45: 222–232.
35. Kuban KC and Gilles FH. Human telencephalic angiogenesis. *Ann Neurol* 1985; 17: 539–548.
36. Sacco M, Meschi M, Regolisti G, et al. The relationship between blood pressure and pain. *J Clin Hypertens (Greenwich)* 2013; 15: 600–605.
37. Girouard H and Iadecola C. Neurovascular coupling in the normal brain and in hypertension, stroke, and Alzheimer disease. *J Appl Physiol (1985)* 2006; 100: 328–335.
38. Boas DA, Jones SR, Devor A, et al. A vascular anatomical network model of the spatio-temporal response to brain activation. *NeuroImage* 2008; 40: 1116–1129.
39. Devor A, Hillman EM, Tian P, et al. Stimulus-induced changes in blood flow and 2-deoxyglucose uptake dissociate in ipsilateral somatosensory cortex. *J Neurosci* 2008; 28: 14347–14357.
40. Crosson B, Ford A, McGregor KM, et al. Functional imaging and related techniques: an introduction for rehabilitation researchers. *J Rehabil Res Dev* 2010; 47: vii–xxxiv.
41. Baran U and Wang RK. Review of optical coherence tomography based angiography in neuroscience. *Neurophotonics* 2016; 3: 010902.
42. Errico C, Pierre J, Pezet S, et al. Ultrafast ultrasound localization microscopy for deep super-resolution vascular imaging. *Nature* 2015; 527: 499–502.
43. De Silva TM and Faraci FM. Microvascular dysfunction and cognitive impairment. *Cell Mol Neurobiol* 2016; 36: 241–258.
44. Vanlandewijck M, He L, Mae MA, et al. A molecular atlas of cell types and zonation in the brain vasculature. *Nature* 2018; 554: 475–480.
45. Mishra A, Reynolds JP, Chen Y, et al. Astrocytes mediate neurovascular signaling to capillary pericytes but not to arterioles. *Nat Neurosci* 2016; 19: 1619–1627.
46. Iadecola C. The neurovascular unit coming of age: a journey through neurovascular coupling in health and disease. *Neuron* 2017; 96: 17–42.
47. Brew N, Walker D and Wong FY. Cerebral vascular regulation and brain injury in preterm infants. *Am J Physiol Regul Integr Comp Physiol* 2014; 306: R773–786.
48. Panfoli I, Candiano G, Malova M, et al. Oxidative stress as a primary risk factor for brain damage in preterm newborns. *Front Pediatr* 2018; 6: 369–369.